Letter

Mechanisms of scrambling and unscrambling of quantum information in the ground state in spin chains: Domain walls, spin flips, and scattering phase shifts

Samudra Sur and Diptiman Sen
Center for High Energy Physics, Indian Institute of Science, Bengaluru 560012, India

(Received 11 December 2023; accepted 7 June 2024; published 9 July 2024)

The out-of-time-order correlator (OTOC) measures the propagation and scrambling of local quantum information. For the transverse field Ising model with open boundaries, the local operator σ^x shows an interesting picture of the ground state OTOC where the local information alternately gets scrambled and then "unscrambled" upon reflection at the ends. Earlier discussions of OTOCs did not explain the physical processes responsible for such scrambling and unscrambling. We explicitly show that in the paramagnetic phase, the scrambling and unscrambling is due to the scattering of a pair of low-energy spin-flip excitations, and extend it to incorporate integrability-breaking interactions. In the ferromagnetic phase these are explained by the motion of a domain-wall excitation, and we find that unscrambling survives up to moderate values of interactions. Thus, in different limits of the system parameters, we provide a simple understanding of the OTOCs, including the unscrambling, in terms of the low-energy excitations like spin flips or domain walls. We mention a system where our results can be experimentally tested.

DOI: 10.1103/PhysRevB.110.L020305

Introduction. The spreading of local quantum information in a quantum many-body system, known as scrambling [1–12], is generally described by the growth of a local operator under time evolution. The front of the operator (or the light cone) is known to spread ballistically [13–17] in lattice systems with a bound on the speed of propagation called the Lieb-Robinson velocity [18]. Quantitatively, scrambling is measured by the real part of the out-of-time-order correlator (OTOC) [19–31], $F(l,t) = \langle W_l(t)V_0W_l(t)V_0\rangle$, where the local operators V and W are at the positions 0 and l, and the expectation is taken in a suitable equilibrium ensemble. Recently, it was found that in noninteracting spin-1/2 chains, the OTOCs for certain operators show scrambling of quantum information inside the light cone [namely, $F(l,t)$ deviates considerably from 1], while for other operators they do not [32,33]. This phenomenon was attributed to the locality or nonlocality of those operators in the Jordan-Wigner (JW) fermionic picture, but without a quantitative explanation. So far, attempts to understand scrambling through OTOCs have been based mainly been on studies of the Heisenberg time-evolution of the local operator using the Baker-Campbell-Hausdorff commutator expansion. In this context, several works [15–17,34–38] in recent times have described the operator spreading in one dimension in terms of a coarse-grained hydrodynamic picture of quasiparticle diffusion. While these explain the ballistic spreading and diffusive broadening of the operator front, an exact mechanism for scrambling in terms of the excitations of the system has been elusive so far. We note here that scrambling is not necessarily a signature of quantum chaos, and OTOC quantifies the degree of scrambling [39,40].

It has been reported in a recent study [33] that the initial local operator starting from one end of the system gets scrambled under time evolution, and again becomes localized after reflection from the other end of the system. We call this effect "unscrambling," which is marked by the value of the OTOC becoming close to 1 again. Interestingly, this feature disappears gradually with increasing interaction strength. It is not well understood yet if the presence or absence of unscrambling is due of the nonintegrability of the system or only because of interactions between the excitations.

In order to understand the mechanism of scrambling and unscrambling in terms of the excitations of the system, we study the ground state OTOC of the longitudinal magnetization (which is nonlocal in terms of Jordan-Wigner fermions) in the transverse field Ising model (TFIM) with and without interactions. The OTOC for JW local operators in the TFIM, which shows only propagation of the front without scrambling, can be evaluated exactly using Wick's theorem. The calculation of the OTOC for JW nonlocal operators (see Fig. 1) in the fermionic language is more tricky and prevents a simple physical understanding of the effects mentioned above. Therefore, we resort to a perturbative approach directly in the spin language. In the paramagnetic (PM) phase of the TFIM, we show that the operator creates spin-flip excitations above the ground state. The scrambling and unscrambling of quantum information happens due to the scattering phase shifts of two spin-flip excitations. In the ferromagnetic (FM) phase, the operator excites domain walls [31] above the ground state which are responsible for the scrambling and unscrambling. Additionally, if interactions are added, the unscrambling in the ground state OTOC fades away. We find that this is due to different reasons in the PM and the FM phases. In the PM phase, even small interactions alter the scattering phase shift significantly from the noninteracting case and obstruct unscrambling. In the FM phase, a comparatively larger interaction is needed to disrupt the unscrambling by creating higher order domain wall excitations. In this Letter, we will provide a detailed quantitative analysis of these mechanisms

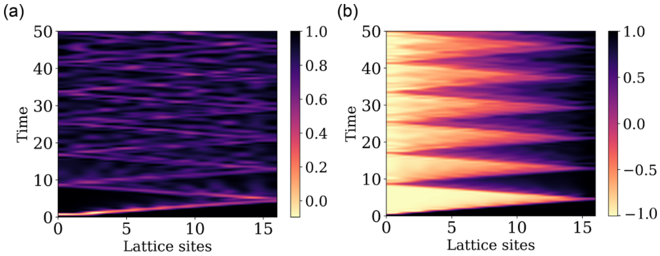

FIG. 1. Spatiotemporal plots of the ground state OTOC for (a) the JW local operator σ^z and (b) the JW nonlocal operator σ^x, at the critical point of the TFIM given in Eq. (1) with $J_x = h = 2$. The σ^z-OTOC F^{zz} shows only light-cone lines of information propagation, while the σ^x-OTOC F^{xx} shows alternating scrambling of quantum information and unscrambling after reflections from the ends. Mixed OTOCs, F^{zx} and F^{xz}, give plots similar to F^{zz} in (a) (see Ref. [41]).

with a comparison of the OTOCs calculated using numerical exact diagonalization and our effective theory of low-energy excitations, and we find an excellent match between the two.

Ground state OTOC. The Hamiltonian of the TFIM is

$$H = -J_x \sum_{n=0}^{L-2} \sigma_n^x \sigma_{n+1}^x - h \sum_{n=0}^{L-1} \sigma_n^z \qquad (1)$$

on a lattice with L sites and open boundaries. As the transverse field h is decreased from a large value, the model exhibits a continuous phase transition from paramagnetic to ferromagnetic at $h = J_x$. We consider the OTOC of the local operator σ^x starting from one end, $F^{xx}(l,t) = \langle \sigma_l^x(t)\sigma_0^x\sigma_l^x(t)\sigma_0^x\rangle$ and analyze it in the PM and FM phases using perturbative treatments for large and small transverse fields, respectively.

Paramagnetic phase: spin-flip excitations. In the paramagnetic phase, at large values of the transverse field, $|h/J_x| \gg 1$, the ground state has all the spins aligned in the direction of the field, $|\uparrow\uparrow\uparrow\cdots\uparrow\rangle_z$ in the σ^z basis. The lowest energy excitations are given by single spin-flips like $|\uparrow\downarrow\uparrow\cdots\uparrow\rangle_z$. In the OTOC, σ_0^x acting on the ground state creates a spin-flip excitation at the left-most (zeroth) site which can then hop through the chain due to the $J_x\sigma_n^x\sigma_{n+1}^x$ term in the Hamiltonian. Subsequently, σ_l^x can either produce a second spin-flip excitation or de-excite the system back to the ground state. Thus, the ground state OTOC is approximately governed by a combination of two processes, one which involves only single spin-flip excitations and the other involving two spin-flips [see Fig. 2(a)]. This becomes clear if we write the OTOC using the intermediate excited states by resolving the identity approximately as $\mathbb{I} \approx |\psi_{GS}\rangle\langle\psi_{GS}| + \sum_q |q\rangle\langle q| + \sum_{q_1,q_2}|q_1,q_2\rangle\langle q_1,q_2| +$ higher order excitations:

$$\begin{aligned}F^{xx}(l,t) \simeq \sum_{q,q'} \Big[&\langle\psi_{GS}|\, e^{iHt}\sigma_l^x\,|q'\rangle\langle q'|\, e^{-iHt}\sigma_0^x\,|\psi_{GS}\rangle \\ &\times \langle\psi_{GS}|e^{iHt}\sigma_l^x\,|q\rangle\langle q|\,e^{-iHt}\sigma_0^x\,|\psi_{GS}\rangle\Big] \\ &+ \sum_{q_1,q_4,q_2<q_3}\Big[\langle\psi_{GS}|e^{iHt}\sigma_l^x\,|q_4\rangle\langle q_4|\,e^{-iHt}\sigma_0^x\,|q_2,q_3\rangle \\ &\times\langle q_2,q_3|e^{iHt}\sigma_l^x\,|q_1\rangle\langle q_1|\,e^{-iHt}\sigma_0^x\,|\psi_{GS}\rangle\Big], \end{aligned} \qquad (2)$$

where $|q\rangle$ and $|q_1,q_2\rangle$ denote the eigenstates of the Hamiltonian with single and two spin-flip excitations, respectively.

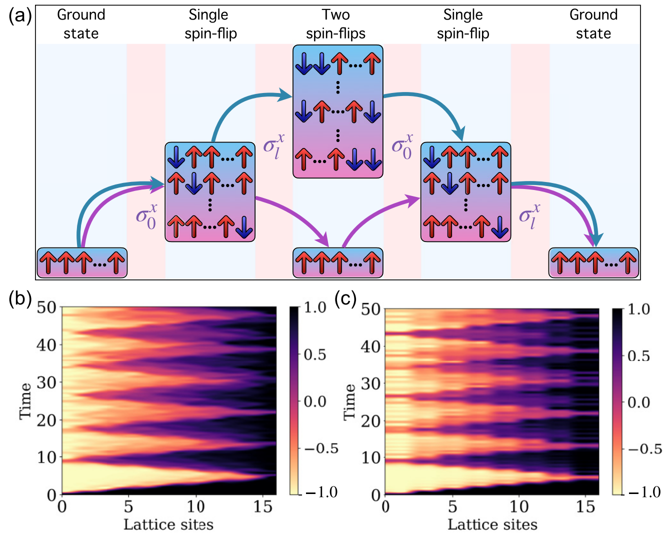

FIG. 2. (a) Schematic of the mechanism of scrambling and unscrambling of $F^{xx}(l,t)$ involving two spin-flip excitations in the paramagnetic phase of the TFIM. (b) $F^{xx}(l,t)$ as obtained from a numerical time evolution for $J_x = 2$ and $h = 4$. (c) $F^{xx}(l,t)$ for the same parameter values obtained using the effective theory of two spin-flip excitations. We see an excellent agreement between plots (b) and (c).

The quantum number q takes the values $0, 1, \ldots, L-1$. We note that it is enough to consider processes up to the second order if J_x/h is small. The matrix elements in Eq. (2) can be evaluated using the energies and wave functions of the excited states $|q\rangle$ and $|q_1,q_2\rangle$. The single spin-flip excitations are described by an effective nearest-neighbor tight-binding model on the L-site lattice with open boundaries. Hence, they have energies $\varepsilon_q = -2J_x\cos(\frac{\pi q}{L+1}) + 2h$ above the ground state, and wave functions $\psi_q(n) = \langle n|q\rangle = \sqrt{2/(L+1)}\sin[\pi(q+1)(n+1)/(L+1)]$, where $|n\rangle = \sigma_n^x|\psi_{GS}\rangle$ denotes the state with a single flipped spin at site n.

While the single-particle eigenstates are solved by considering the problem of a particle in a box on a lattice, the case of two spin flips is more subtle. The two spin flips should be on separate sites and follow commutation relations, making it a system with two hard-core bosons. Due to the indistinguishability, we can write the wave function for this state as $\psi_{q_1,q_2}(n_1,n_2) = \langle n_1,n_2|q_1,q_2\rangle = \psi_{q_1}(n_1)\psi_{q_2}(n_2) - \psi_{q_2}(n_1)\psi_{q_1}(n_2)$, where $|n_1,n_2\rangle$ denotes the state with two spin flips at sites n_1 and n_2, and we choose $n_1 < n_2$. The energy of this state is the sum of two single-particle energies, $\varepsilon_{q_1,q_2} = \varepsilon_{q_1} + \varepsilon_{q_2}$. Finally, we arrive at [41]

$$\begin{aligned}F^{xx}(l,t) \simeq &\sum_{q,q'} e^{-i(E_q+E_{q'})t}\psi_q(l)\psi_q(0)\psi_{q'}(l)\psi_{q'}(0) \\ &+ \sum_{q_1,q_4,q_2<q_3} e^{-i(E_{q_1}+E_{q_4}-E_{q_2}-E_{q_3})t}\psi_{q_1}(0)\psi_{q_4}(l) \\ &\times\sum_{n_1}\psi_{q_1}(n_1)[\theta(n_1-l)\psi_{q_2,q_3}(l,n_1) \\ &+\theta(l-n_1)\psi_{q_2,q_3}(n_1,l)] \\ &\times\sum_{n_2}\psi_{q_4}(n_2)\psi_{q_2,q_3}(0,n_2). \end{aligned} \qquad (3)$$

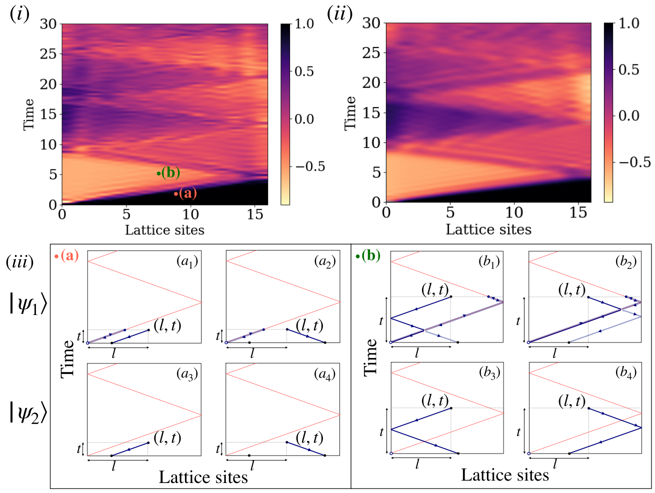

FIG. 3. Plots of $F^{xx}(l,t)$ for the interacting TFIM with $J_x = 2$, $h = 8$, $J_z = 1.8$ obtained from (i) exact numerics and (ii) the analysis using two spin-flip excitations. Two points (a) and (b) are shown in plot (i). The value of J_z is such that a region which showed scrambling in the noninteracting case now shows OTOC close to 1. (iii) The point (a) (left panel) corresponds to a region where there is no scattering between the states $|\psi_1\rangle$ and $|\psi_2\rangle$, while at point (b) (right panel) there is a scattering event between the two excitations in $|\psi_1\rangle$.

We evaluate this expression exactly and contrast this with the $F^{xx}(l,t)$ calculated using exact numerical time evolution in Figs. 2(b) and 2(c). The striking agreement confirms that spin-flip excitations indeed provide the mechanism responsible for the scrambling of quantum information and the unscrambling after a reflection when h is large. Interestingly, this analysis agrees quite well with the exact result even if h is not much larger than J_x. In fact, the plot for OTOC looks qualitatively the same for $h = J_x$ [Fig. 1(b)] and $h > J_x$ [Fig. 2(b)], although an analysis in terms of spin-flip excitations is not expected to hold near the critical point.

Interactions in the presence of large field. We now look at the OTOC in the PM phase in the presence of an integrability-breaking interaction term given by $J_z \sum_n \sigma_n^z \sigma_{n+1}^z$. The full Hamiltonian is $H = -J_x \sum_{n=0}^{L-2} \sigma_n^x \sigma_{n+1}^x - h \sum_{n=0}^{L-1} \sigma_n^z + J_z \sum_{n=0}^{L-2} \sigma_n^z \sigma_{n+1}^z$. When $|h/J_x| > 1$, a small value of J_z can significantly change the plot of $F^{xx}(l,t)$, as we see in Fig. 3(a). As usual, the local quantum information starts scrambling after σ_0^x acts at one end. However, we do not see any unscrambling after reflection, unlike in the model without interactions. As time progresses further, the local information always stays scrambled and never becomes localized to a few sites. This can also be explained using a simple picture of two-spin flips. We need to modify Eq. (3) to account for two-spin flip states in the presence of interactions and evaluate it numerically. The wave functions for the two-spin flip state $\psi_{q_1,q_2}(n_1,n_2)$ are replaced by two-body eigenstates calculated numerically by considering an effective tight-binding model with two hard-core bosons with a nearest-neighbor density-density interaction J_z. The OTOC calculated in this way shows fairly good agreement with the plots obtained using exact numerics even with interactions. We contrast the two plots in Figs. 3(i) and 3(ii) for the parameter values $J_x = 2$, $h = 8$, and $J_z = 1.8$.

There is a simple space-time picture in terms of the spin-flip excitations which allows us to intuitively understand the plots of $F^{xx}(l,t)$ when h is large. This is shown in Fig. 3(iii), and it will be discussed below in the Appendix.

Similar effects are observed if we consider the integrable but interacting XXZ spin-1/2 model in a transverse field. Namely, for the Hamiltonian, $H' = -J \sum_{n=0}^{L-2} \sigma_n^x \sigma_{n+1}^x - J \sum_{n=0}^{L-2} \sigma_n^y \sigma_{n+1}^y - h \sum_{n=0}^{L-1} \sigma_n^z + J_z \sum_{n=0}^{L-2} \sigma_n^z \sigma_{n+1}^z$, the OTOC shows a similar behavior including the absence of unscrambling as compared to the noninteracting XX model without the J_z term (see Ref. [41]). Therefore, a similar analysis in terms of the low-energy excitations holds true for the XXZ spin-1/2 model as well, implying that the absence of unscrambling is not related to the the integrability or nonintegrability of the model.

Ferromagnetic phase: domain walls. We now discuss the scrambling in the FM phase of the TFIM. For very small h, the ground states are the degenerate states $|I\rangle = |\uparrow\uparrow \cdots \uparrow\rangle_x$ and $|II\rangle = |\downarrow\downarrow \cdots \downarrow\rangle_x$ in the σ^x basis. The model has a Z_2 spin-flip symmetry, but the ground states spontaneously break this and the true ground states are the superpositions $|+\rangle = (|I\rangle + |II\rangle)/\sqrt{2}$ and $|-\rangle = (|I\rangle - |II\rangle)/\sqrt{2}$ corresponding to even and odd fermion parity, respectively. Setting $J_x = 1$ and taking h small, a perturbative expansion up to first order in h [41] yields the modified ground states expressed in a product form $|I'\rangle = |(\uparrow + \frac{h}{2} \downarrow)_0 (\uparrow + \frac{h}{4} \downarrow)_1 \cdots (\uparrow + \frac{h}{2} \downarrow)_{L-1}\rangle_x$ and $|II'\rangle = |(\downarrow + \frac{h}{2} \uparrow)_0 (\downarrow + \frac{h}{4} \uparrow)_1 \cdots (\downarrow + \frac{h}{2} \uparrow)_{L-1}\rangle_x$ (up to a normalization constant), where the subscripts denote the site indices. The lowest energy excitations are the two types of domain walls, namely $|m+1/2, I\rangle$ and $|m+1/2, II\rangle$, where the label $m+\frac{1}{2}$ implies that the domain wall is situated between the mth and $(m+1)$th sites, and I (II) denotes that all the spins on the left of the domain wall are down (up). Here m can take values from 0 to $L-2$. For example, $|0+1/2, I\rangle = |\downarrow\uparrow\uparrow \cdots \uparrow\rangle_x$ denotes the state with a domain wall between the first and second spins. Now, σ_0^x acting on the state $|I'\rangle$ creates the domain-wall state $|0+1/2, I\rangle$ with an amplitude h to leading order. Under time evolution, this domain wall can move through the lattice with one less site due to the $h \sum \sigma_n^z$ term in the Hamiltonian, allowing us to construct domain-wall eigenstates with a quantum number label κ. Accordingly, domain-wall states have an energy dispersion $\epsilon_{\kappa,\alpha} = -2h\cos[\pi(\kappa+1)/L] + 2J_x$ above the ground state, and a wave function $\phi_{\kappa,\alpha}(m) = \langle m+1/2, \alpha \mid \kappa, \alpha\rangle = \sqrt{2/L}\sin[\pi(\kappa+1)(m+1)/L]$, where $\kappa = 0, 1, \cdots, L-2$, and α can be I or II. Subsequently, σ_l^x for $l \neq 0$ does not create or destroy the domain-wall excitation but only measures if the spin is up or down in the x basis. However, it changes the parity of the domain-wall excitation. The remaining σ_0^x and σ_l^x operators first de-excite the domain wall to a ground state with the opposite parity, and then returns it to the ground state we started with. In short, as the domain moves from one end to the other end, it leaves flipped spins behind along its trajectory. This is then measured by the operator σ_l^x at different times. The entire mechanism is described schematically in Fig. 4(a). We have a different situation when $l = 0$, as the four σ_0^x operators sequentially excite and de-excite between the ground

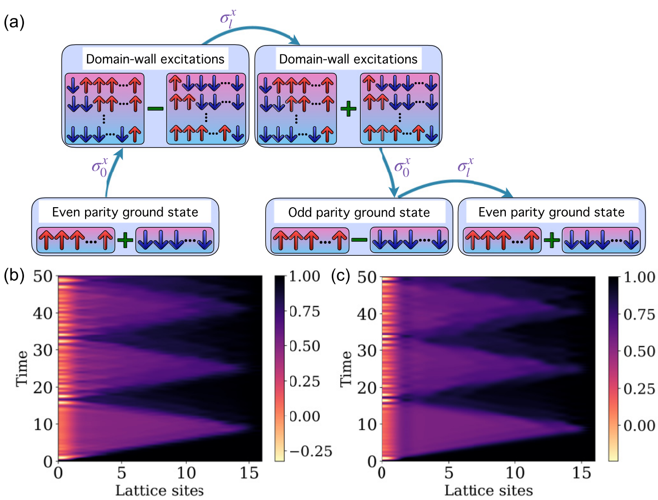

FIG. 4. (a) Schematic of the mechanism of domain-wall assisted scrambling and unscrambling in the ordered phase of the TFIM. Plots of $F^{xx}(l,t)$ for $J_x = 2$ and $h = 1$ obtained by using (b) exact numerics in the ordered phase, and (c) the analysis of domain-wall excitations described in the text. These agree remarkably well.

state and a domain-wall state, resulting in a different value of the OTOC at the edge.

We now present a semianalytical treatment of domain-wall dynamics to quantitatively understand scrambling and unscrambling. To this end, we construct the σ_n^x operators at all sites which is perturbatively correct up to order h in the subspace consisting only of the ground state and single domain-wall states. The operator σ_0^x has nontrivial matrix elements only in the subspace of states $\{|I'\rangle, |0+1/2, I\rangle\}$ and $\{|II'\rangle, |0+1/2, II\rangle\}$. On the other hand, σ_{L-1}^x has nontrivial elements in the subspaces spanned by the states $\{|I'\rangle, |L-2+1/2, II\rangle\}$ and $\{|II'\rangle, |L-2+1/2, I\rangle\}$. The σ_l^x for all other sites are diagonal and have trivial matrix elements (± 1) up to order h as they only determine whether the spin is up or down. The Hamiltonian then has a simple structure with only the ground state energy along the diagonal in the ground state basis and a tight-binding structure in the subspace of domain walls. Since the Hamiltonian only appears in the exponential in time evolution, we do not need to consider the matrix elements between the ground states and the domain walls to the lowest order.

The effective forms of σ_n^x and the Hamiltonian H in the subspace spanned by the states $|I'\rangle$, $|II'\rangle$, and $|m+1/2, I\rangle$, $|m+1/2, II\rangle$, where $m = 0, \cdots, L-2$, are defined as X_n and $\mathcal{H}$ (see Ref. [41]). The OTOC can then be written as $F^{xx}(l,t) \simeq \frac{1}{2}\langle I' + II'|\, e^{i\mathcal{H}t} X_l e^{-i\mathcal{H}t} X_0 e^{i\mathcal{H}t} X_l e^{-i\mathcal{H}t} X_0\, |I' + II'\rangle$, which is correct up to order h^2. The plots of $F^{xx}(l,t)$ using exact numerics and our analysis agree very well as shown in Figs. 4(b) and 4(c). Moreover, in both the plots we observe the reflection of scrambled quantum information happening slightly before it reaches the other end, which validates that it is indeed governed by domain-wall excitations (which are defined midway between sites).

Interactions in the presence of small field. In the FM phase, the introduction of a small interaction J_z (relative to J_x) does

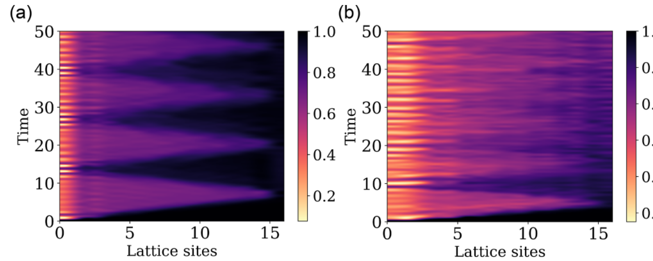

FIG. 5. $F^{xx}(l,t)$ showing a pronounced unscrambling effect for (a) $J_x = 2,\ h = 1,\ J_z = 0.5$, while for (b) $J_x = 2,\ h = 1,\ J_z = 1$, it shows much less unscrambling.

not alter the qualitative features of the $F^{xx}(l,t)$ much. We can see scrambling and unscrambling much as in the case without interactions. A small J_z also contributes to the dynamics of a domain wall by making it hop by two sites, in contrast to the transverse field h which leads to hopping by one site. Therefore, the presence of a small interaction effectively only changes the dispersion of the domain walls to $E_k = -2h\cos k + 2J_z\cos(2k)$. The group velocity is then given by $v_k = dE_k/dk = 2h\sin k - 4J_z\sin(2k)$. Since the light-cone velocity is the maximum group velocity of the quasiparticles, the interacting model [Fig. 5(a)] shows a different light-cone velocity than its noninteracting counterpart.

If J_z is increased further, we find that the unscrambling starts to go away. Roughly, this happens around $J_z/J_x \gtrsim 0.4$, as observed numerically. Figure 5(b) shows the absence of unscrambling for the parameter values $J_x = 2,\ h = 1,\ J_z = 1$. It can be reasonably expected that for such values of J_z, the perturbative expansion starting from the states $|I\rangle$ and $|II\rangle$ will no longer be accurate. Furthermore, the assumption that only the lowest-order excitations are responsible for information scrambling also becomes a gross oversimplification. To explain the absence of unscrambling when J_z is comparable with J_x, one needs to account for higher-order excitations like dynamics of three or more domain walls.

Conclusion. To summarize, we have studied the propagation of local quantum information in a spin-$1/2$ chain with open boundary conditions using ground state OTOCs of σ^z and σ^x operators which are local and nonlocal in terms of JW fermions, respectively. While both σ^z and σ^x OTOCs show light-cone-like propagation, only the σ^x OTOC shows scrambling within the light cone, in agreement with earlier results. In addition, we discover remarkable unscramblings and scramblings of the σ^x OTOC after repeated reflections from the ends. We have provided an analytical understanding of both scrambling and unscrambling deep in the PM phase (when the transverse field h is large) and in the FM phase (when the XX coupling J_x is large) in terms of the low-energy excitations, namely, spin flips when h is large and domain walls when J_x is large. When an interaction between the JW fermions (ZZ coupling) is added, the unscrambling effect becomes weaker. In the PM phase, even relatively weak interactions significantly change the scattering phase shift for two spin flips and thereby reduces the unscrambling. In the FM phase, stronger interactions are required to destroy unscrambling and it occurs due the the creation of multiple domain-wall excitations. Interestingly, we find that in the absence of interactions, the scrambling and unscrambling are visible in the OTOCs even for the infinite-temperature ensemble [41]. This indicates that in a noninteracting system, the mechanisms of operator spreading can be understood by the dynamics of one or two excitations even if we begin with excited eigenstates.

We conclude by pointing out a recent experimental measurement of the OTOC [42] at finite temperature which, as the authors suggest, can also be performed for the ground state. In this paper, finite temperature OTOCs of the transverse field Ising model are studied for a trapped linear chain of $^{171}\mathrm{Yb}^{+}$ ions by creating a thermofield double state and then looking at its time evolution. We believe that a similar route can be followed to experimentally study the dynamics of low-energy excitations through the ground state OTOCs of the spin chains discussed in our work.

Acknowledgments. S.S. thanks MHRD, India for financial support through the PMRF. D.S. acknowledges funding from SERB, India (JBR/2020/000043).

Appendix on a space-time picture for the OTOC plots. We will present here a space-time picture to understand the plots of $F^{xx}(l,t)$ when the transverse field h is large. The expression for the OTOC can be rewritten as $F^{xx}(l,t) = \langle\psi_{GS}|\, e^{iHt}\sigma_l^x e^{-iHt}\sigma_0^x e^{iHt}\sigma_l^x e^{-iHt}\sigma_0^x\,|\psi_{GS}\rangle = \langle\psi_2|\psi_1\rangle$, where $|\psi_1\rangle$ and $|\psi_2\rangle$ are both states with one particle (spin-flip) and are defined as $|\psi_1\rangle = \sigma_0^x e^{iHt}\sigma_l^x e^{-iHt}\sigma_0^x\,|\psi_{GS}\rangle$ and $|\psi_2\rangle = e^{iHt}\sigma_l^x e^{-iHt}\,|\psi_{GS}\rangle$. The state $|\psi_1\rangle$ can be interpreted as follows. Starting from the right, the first σ_0^x operator creates a spin flip at the left-most site which then propagates with some velocity for a time t (due to e^{-iHt}). Next, a second spin flip is created at site l. The two flipped spins then propagate back in time (due to e^{iHt}) to $t = 0$ which involves zero, one, or more scatterings between them depending on the position l and time t. Finally, at $t = 0$ one of the spin flips is annihilated at site $l = 0$ to produce a state with only one spin flip. In contrast, $|\psi_2\rangle$ has a simpler interpretation. It involves a single spin flip which is created at position l and time t on the time-evolved ground state, and which then propagates back in time to $t = 0$. The inner product $\langle\psi_2|\psi_1\rangle$ then depends on the scattering phase shift in the state $|\psi_1\rangle$ with respect to state $|\psi_2\rangle$.

Some assumptions are now required to compute the OTOC using scattering phase shifts. First, even though we are considering a system with open boundaries, we will assume that the system is large enough such that away from the edge, the momentum q is a good quantum number. Second, we approximate a spin-flip excitation to be a quasiparticle with a single momenta q_0 with the largest possible group velocity given by the Lieb-Robinson bound, although actually it is a superposition of many momentum states around q_0. The entire region in the plot of the OTOC can now be divided into regions according to the number of scatterings between a pair of quasiparticles with momenta q_0 and $-q_0$ in the state $|\psi_1\rangle$. The real part value of the OTOC in each region is approximately constant and is given by the real part of the scattering phase shift obtained from the two-particle Bethe ansatz [41].

The scrambling and unscrambling for the TFIM without interactions [Fig. 2(b)], given by the successive dark (OTOC close to 1) and bright (OTOC close to -1) regions can be now understood as regions having an even and odd number of scatterings respectively starting from the lowest dark region (where there is no scattering). In the absence of interactions, every scattering event changes the phase by $e^{i\theta} = -1$. For the interacting model, the absence of unscrambling occurs due to the deviation of scattering phase shifts from -1 due to J_z. However, we note that at much later times the contributions from excitations not corresponding to the largest group velocity become significant and they alter the value of the OTOC obtained from the estimate given by scattering phase shifts of two excitations at momenta $\pm q_0$.

To illustrate this, we have chosen two points (a) and (b) in the OTOC plots in Fig. 3(i) where point (a) is in a region of no scrambling and (b) is in a region of scrambling before any reflection. We now consider the schematic shown in Fig. 3(iii). The red lines are guides to the eye for the light-cone front. Then $|\psi_1\rangle$ at (a) is given by a superposition of one-particle states shown in (a_1) and (a_2) involving the dynamics of two excitations created respectively at space-time coordinates (0,0) and (l,t) and one of them is finally annihilated again at (0,0). By contrast, $|\psi_2\rangle$ at (a) is a superposition of one-particle states shown in (a_3) and (a_4) involving only a single excitation. Since there is no scattering event for point (a), $F^{xx} = \langle\psi_2|\psi_1\rangle = 1$. For point (b), $|\psi_1\rangle$ is a superposition of states shown in (b_1) and (b_2), and $|\psi_2\rangle$ is a superposition of states shown in (b_3) and (b_4). In contrast to point (a), we have one scattering phase shift between two excitations in the state $|\psi_1\rangle$ with respect to the state $|\psi_2\rangle$. The inner product of the two states brings out the scattering phase shift, which, for a pair of noninteracting hard-core bosons, is equal to -1. This explains the value of $F^{xx}(l,t)$ in the first scrambled region in the TFIM. For the interacting case also it has a value close to -1. Subsequently, for larger times the scrambled and unscrambled regions have values of $F^{xx}(l,t)$ given by the total number of scattering events multiplied by the phase shift of one scattering event. In Figs. 3(i) and 3(ii) we have considered a J_z so that the region corresponding to three scattering events has $F^{xx}(l,t)$ close to 1, which, for the noninteracting case, would have been close to -1.

[1] D. A. Roberts and B. Swingle, Lieb-Robinson bound and the butterfly effect in quantum field theories, Phys. Rev. Lett. **117**, 091602 (2016).

[2] P. Hosur, X.-L. Qi, D. A. Roberts, and B. Yoshida, Chaos in quantum channels, J. High Energy Phys. 02 (2016) 004.

[3] B. Swingle and D. Chowdhury, Slow scrambling in disordered quantum systems, Phys. Rev. B **95**, 060201(R) (2017).

[4] A. A. Patel, D. Chowdhury, S. Sachdev, and B. Swingle, Quantum butterfly effect in weakly interacting diffusive metals, Phys. Rev. X **7**, 031047 (2017).

[5] M. Campisi and J. Goold, Thermodynamics of quantum information scrambling, Phys. Rev. E **95**, 062127 (2017).

[6] E. Iyoda and T. Sagawa, Scrambling of quantum information in quantum many-body systems, Phys. Rev. A **97**, 042330 (2018).

[7] S. Pappalardi, A. Russomanno, B. Žunkovič, F. Iemini, A. Silva, and R. Fazio, Scrambling and entanglement spreading in long-range spin chains, Phys. Rev. B **98**, 134303 (2018).

[8] M. J. Klug, M. S. Scheurer, and J. Schmalian, Hierarchy of information scrambling, thermalization, and hydrodynamic flow in graphene, Phys. Rev. B **98**, 045102 (2018).

[9] W. Kirkby, J. Mumford, and D. H. J. O'Dell, Quantum caustics and the hierarchy of light cones in quenched spin chains, Phys. Rev. Res. **1**, 033135 (2019).

[10] Y. Alavirad and A. Lavasani, Scrambling in the Dicke model, Phys. Rev. A **99**, 043602 (2019).

[11] S. Sahu, S. Xu, and B. Swingle, Scrambling dynamics across a thermalization-localization quantum phase transition, Phys. Rev. Lett. **123**, 165902 (2019).

[12] S. Sur and V Subrahmanyam, Information scrambling and redistribution of quantum correlations through dynamical evolution in spin chains, Quantum Info. Proc. **21**, 301 (2022).

[13] D. J. Luitz and Y. B. Lev, Information propagation in isolated quantum systems, Phys. Rev. B **96**, 020406(R) (2017).

[14] A. Bohrdt, C. B. Mendl, M. Endres, and M. Knap, Scrambling and thermalization in a diffusive quantum many-body system, New J. Phys. **19**, 063001 (2017).

[15] V. Khemani, A. Vishwanath, and D. A. Huse, Operator spreading and the emergence of dissipative hydrodynamics under unitary evolution with conservation laws, Phys. Rev. X **8**, 031057 (2018).

[16] T. Rakovszky, F. Pollmann, and C. W. von Keyserlingk, Diffusive hydrodynamics of out-of-time-ordered correlators with charge conservation, Phys. Rev. X **8**, 031058 (2018).

[17] C. W. von Keyserlingk, T. Rakovszky, F. Pollmann, and S. L. Sondhi, Operator hydrodynamics, OTOCs, and entanglement growth in systems without conservation laws, Phys. Rev. X **8**, 021013 (2018).

[18] E. H. Lieb and D. W. Robinson, The finite group velocity of quantum spin systems, Commun. Math. Phys. **28**, 251 (1972).

[19] A. I. Larkin and Y. N. Ovchinnikov, Quasiclassical method in the theory of superconductivity, JETP **28**, 1200 (1969).

[20] S. H. Shenker and D. Stanford, Black holes and the butterfly effect, J. High Energy Phys. 03 (2014) 067.

[21] J. Maldacena, S. H. Shenker, and D. Stanford, A bound on chaos, J. High Energy Phys. 08 (2016) 106.

[22] B. Dóra and R. Moessner, Out-of-time-ordered density correlators in Luttinger liquids, Phys. Rev. Lett. **119**, 026802 (2017).

[23] H. Shen, P. Zhang, R. Fan, and H. Zhai, Out-of-time-order correlation at a quantum phase transition, Phys. Rev. B **96**, 054503 (2017).

[24] M. Heyl, F. Pollmann, and B. Dóra, Detecting equilibrium and dynamical quantum phase transitions in Ising chains via out-of-time-ordered correlators, Phys. Rev. Lett. **121**, 016801 (2018).

[25] J.-H. Bao and C.-Y. Zhang, Out-of-time-order correlators in the one-dimensional XY model, Commun. Theor. Phys. **72**, 085103 (2020).

[26] M. McGinley, A. Nunnenkamp, and J. Knolle, Slow growth of out-of-time-order correlators and entanglement entropy in integrable disordered systems, Phys. Rev. Lett. **122**, 020603 (2019).

[27] J. Riddell and E. S. Sørensen, Out-of-time ordered correlators and entanglement growth in the random-field XX spin chain, Phys. Rev. B **99**, 054205 (2019).

[28] C. B. Dağ, K. Sun, and L.-M. Duan, Detection of quantum phases via out-of-time-order correlators, Phys. Rev. Lett. **123**, 140602 (2019).

[29] S. Zamani, R. Jafari, and A. Langari, Out-of-time-order correlations and floquet dynamical quantum phase transition, Phys. Rev. B **105**, 094304 (2022).

[30] R. K. Shukla, G. K. Naik, and S. K. Mishra, Out-of-time-order correlation and detection of phase structure in Floquet transverse Ising spin system, Europhys. Lett. **132**, 47003 (2020).

[31] P. Suchsland, B. Douot, K. Khemani, and R. Moessner, Dynamical correlations and domain wall relocalisation in transverse field Ising chains, arXiv:2207.09502

[32] C.-J. Lin and O. I. Motrunich, Out-of-time-ordered correlators in a quantum Ising chain, Phys. Rev. B **97**, 144304 (2018).

[33] S. Sur and D. Sen, Effects of topological and non-topological edge states on information propagation and scrambling in a Floquet spin chain, J. Phys.: Condens. Matter **36**, 125402 (2024).

[34] S. Gopalakrishnan, D. A. Huse, V. Khemani, and R. Vasseur, Hydrodynamics of operator spreading and quasiparticle diffusion in interacting integrable systems, Phys. Rev. B **98**, 220303(R) (2018).

[35] A. Nahum, S. Vijay, and J. Haah, Operator spreading in random unitary circuits, Phys. Rev. X **8**, 021014 (2018).

[36] U. Agrawal, S. Gopalakrishnan, and R. Vasseur, Generalized hydrodynamics, quasiparticle diffusion, and anomalous local relaxation in random integrable spin chains, Phys. Rev. B **99**, 174203 (2019).

[37] J. Lopez-Piqueres, B. Ware, S. Gopalakrishnan, and R. Vasseur, Operator front broadening in chaotic and integrable quantum chains, Phys. Rev. B **104**, 104307 (2021).

[38] T. Zhou, A. Guo, S. Xu, X. Chen, and B. Swingle, Hydrodynamic theory of scrambling in chaotic long-range interacting systems, Phys. Rev. B **107**, 014201 (2023).

[39] T. Xu, T. Scaffidi, and X. Cao, Does scrambling equal chaos? Phys. Rev. Lett. **124**, 140602 (2020).

[40] N. Dowling, P. Kos, and K. Modi, Scrambling is necessary but not sufficient for chaos, Phys. Rev. Lett. **131**, 180403 (2023).

[41] See Supplemental Material at http://link.aps.org/supplemental/10.1103/PhysRevB.110.L020305 for the derivation of Eq. (3), perturbative ground state for small h, matrix forms for the σ^x operators, two-body scattering phase shift, absence of unscrambling in XXZ model, scrambling and unscrambling in OTOC in a non-interacting system, and OTOC for mixtures of σ^x and σ^z operators.

[42] A. M. Green, A. Elben, C. H. Alderete, L. K. Joshi, N. H. Nguyen, T. V. Zache, Y. Zhu, B. Sundar, and N. M. Linke, Experimental measurement of out-of-time-ordered correlators at finite temperature, Phys. Rev. Lett. **128**, 140601 (2022).